Journal of Alloys and Compounds 489 (2010) 188–194

Contents lists available at ScienceDirect

Journal of Alloys and Compounds

journal homepage: www.elsevier.com/locate/jallcom

Densification behavior of nanocrystalline W–Ni–Fe composite powders prepared by sol-spray drying and hydrogen reduction process

J.L. Fan*, X. Gong, B.Y. Huang, M. Song, T. Liu, J.M. Tian

State Key Laboratory for Powder Metallurgy, Central South University, Changsha, 410083, PR China

ARTICLE INFO

Article history:
Received 20 July 2009
Received in revised form 8 September 2009
Accepted 9 September 2009
Available online 16 September 2009

Keywords:
Nanocrystalline composite powders
93W–4.9Ni–2.1Fe
Yttrium
Densification
Liquid-phase sintering

ABSTRACT

This paper studied the densification behavior of nanocrystalline composite powders of 93W–4.9Ni–2.1Fe (wt.%) and 93W–4.9Ni–2.1Fe–0.03Y synthesized by sol-spray drying and hydrogen reduction process. The X-ray diffraction (XRD) analysis showed that γ-(Ni, Fe) phase was formed in the final obtained powders. Powders morphology characterized by scanning electron microscope (SEM) showed that the 93W–4.9Ni–2.1Fe nanocrystalline composite powders exhibited larger agglomeration and grain size compared with the 93W–4.9Ni–2.1Fe–0.03Y nanocrystalline composite powders. Both kinds of green compacts can obtain full density if sintered at 1410 °C for 1 h. When sintering temperature was above 1410 °C, the sintering density for both compacts decreased rapidly. In addition, the sintering density, densification rate and grain coarsening rate of 93W–4.9Ni–2.1Fe compacts were higher than those of 93W–4.9Ni–2.1Fe–0.03Y. The effect of trace yttrium on the densification behavior of nanocrystalline composite powders was also discussed.

1. Introduction

Tungsten heavy alloys (WHAs) are two-phase composites consisting of nearly spherical tungsten particles embedded homogeneously in a ductile matrix with low melting point, such as nickel, iron, copper and cobalt [1–3]. Due to the outstanding combination of the properties related to the bcc tungsten phase and fcc matrix, such as high mechanical properties, thermal conductivity and good corrosion resistance, WHAs are widely used in light bulbs filaments, radiation shields, vibration dampers, kinetic energy penetrators and rocket nozzles in space crafts [4–6]. WHAs are usually fabricated by liquid-phase sintering (LPS) process from micron-sized W–Ni–Fe elemental powder mixtures [7,8], and the obtained tungsten grain size is typically about 20–50 μm in diameter. To date, many techniques have been developed to fabricate these alloys, such as solid-phase sintering or LPS of elemental powders, solid-phase sintering of mechanical alloying powders, metal injection molding and microwave sintering [9–13].

It is well known that fine-grained materials provide many attractive properties including high strength, hardness, toughness and good ductility at low temperature according to Hall–Petch relationship. In particular, the propensity to adiabatic shear deformation of WHAs is related to high strain rates and shear localization, which strongly depends on the grain structures [14]. Hence, obtaining a fine-grained microstructure of WHAs attracts continual interests [15]. Previously, oxide dispersion strengthening (ODS) was proved to be an effective method to refine the grain size of WHAs [16–19]. At present, the grain refinement by controlling the sintering process of nanocrystalline composite powders has attracted increased attentions [20]. The preparation of nanocrystalline W–Ni–Fe composite powders is a primary step for the production of the fine-grained WHAs, since the powder properties remarkably affect the subsequent pressing and densification processes. In addition, sintering densification of nanocrystalline composite powders is a critical step to obtain full density and small grain-sized microstructures, which may be different from the densification behavior of the conventional microscaled powders. In our previous work [20], the preparation of the nanosized W–Ni–Fe powders by the sol-spray drying technique has been investigated. That paper focused on the characterization of the nanosized powders. The sintering behavior and the effect of trace yttria particles (added into the prepared nanosized powders and then mixed by ball milling) on the mechanical properties of the sintered alloys were only discussed briefly.

In this work, sol-spray drying and hydrogen reduction process were preferentially used to prepare nanocrystalline W–Ni–Fe composite powders, since this technique can avoid the introduction of the detrimental impurities, and most importantly, can obtain a product with homogeneous composition distribution. The sintering behavior of the nanocrystalline composite powders at various temperatures and holding times was systematically investigated. In addition, the effects of trace yttrium addition (added as yttrium nitrate, differing from the addition of yttria particles) on the densification behavior of nanocrystalline composite powders and the

---

* Corresponding author. Tel.: +86 731 88836652; fax: +86 731 8710855.
E-mail address: fjl@mail.csu.edu.cn (J.L. Fan).

0925-8388/$ – see front matter © 2009 Published by Elsevier B.V.
doi:10.1016/j.jallcom.2009.09.050

mechanical properties of the sintered alloys have been systematically studied. It should be noted that the highly active yttrium can react with some elements during the sintering process, and thus affect the densification behavior.

2. Experimental procedures

The raw materials used in the synthesis of nanocrystalline 93W–4.9Ni–2.1Fe and 93W–4.9Ni–2.1Fe–0.03Y composite powders were ammonium metatungstate (purity > 99.5%), $Ni(NO_3)_2{\cdot}6H_2O$ (analytically pure), $Fe(NO_3)_3{\cdot}9H_2O$ (analytically pure) and $Y(NO_3)_3{\cdot}6H_2O$ (analytically pure). According to the stoichiometric ratios, aqueous solution containing W, Ni and Fe salts were prepared by dissolving the solid metal salts into the deionized water with constant stirring. In order to avoid precipitation, a certain amount of PEG-2000 was added into the aqueous solution. Then, nanocrystalline composite powders were obtained by a multi-step process, consisting of sol-spray drying of the precursor solution at 250–350 °C with a solution feed rate of 40–50 ml/min, calcining at 600 °C for 2 h and subsequent reducing by two-step hydrogen reduction process (at 450 °C for 1.5 h and then 850 °C for 1.5 h) in flowing hydrogen atmosphere (dew point of −40 °C). The nanocrystalline 93W–4.9Ni–2.1Fe composite powders with 0.03 wt.% yttrium addition was prepared by the same processes as mentioned above. Since only an imperceptible amount of yttrium exists in the original aqueous solution, the influence of yttrium addition on stoichiometric ratios of the final as-received alloys was negligible.

The nanocrystalline composite powders were die-pressed under 400 MPa for 1 min to form I-shaped samples and the green compacts have a relative density of about 40%. Then, the green compacts were sintered in molybdenum wire furnace under flowing hydrogen atmosphere (dew point of −40 °C) at 900–1460 °C for different holding time. The heating rate was 5 °C/min and the cooling rate to room temperature was 10 °C/min. It should be noted that the present work focused on the densification behavior of the nanocrystalline composite powders and all the obtained data were based on the sintered alloys. The effects of the heat treatment on the microstructures and mechanical behaviors of the sintered compacts will be studied in the future.

The obtained nanocrystalline composite powders were analysed by X-ray diffraction technique (XRD, D/max 2550/Japan). The powders morphology and the sintered compacts were characterized by scanning electron microscope (SEM, JSM-5600LV) and transmission electron microscope (TEM, JEM-200CX). The densities of the sintered compacts were measured by Archimedes' principle. A Nitrogen/Oxygen/Hydrogen Determination (TCH-600, USA) was employed to determine the oxygen contents in the sintered alloys. Hardness of the sintered compacts was determined by means of digital microhardness tester (HXD-1000T).

3. Results and discussion

3.1. Characteristics of nanocrystalline W–Ni–Fe composite powders

Fig. 1 compares the XRD patterns of the nanocrystalline 93W–4.9Ni–2.1Fe and 93W–4.9Ni–2.1Fe–0.03Y composite powders. It can be seen that only one set of the sharp peaks belonging to bcc-structured tungsten phase are present. However, relatively weak peaks corresponding to γ-(Ni, Fe) phase are also observed in the XRD patterns, indicating that Ni–Fe solid solution formed during sol-spray drying and hydrogen reduction process. This means that composite powders are well synthesized by this method. The products are essentially pure W, Ni and Fe without any detectable oxide phases or other impurities that may come from the raw materials or the following preparation processes. The oxygen contents are 0.059 wt.% for nanocrystalline 93W–4.9Ni–2.1Fe composite powders and 0.23 wt.% for nanocrystalline 93W–4.9Ni–2.1Fe–0.03Y composite powders, respectively. It is emphasized that impurities in 93W–4.9Ni–2.1Fe powders, especially oxygen contents, have been effectively controlled during the fabrication process. However, oxygen contents are very high in 93W–4.9Ni–2.1Fe–0.03Y powders due to the strong affinity between yttrium and oxygen. It should be noted that the peaks of yttrium-containing phase are not observed in the patterns as the result of small amount of yttrium additions. The grain sizes of these nanocrystalline composite powders are determined from XRD patterns by applying the Scherrer equation [21] based on no lattice distortion:

$$d = \frac{0.9\lambda}{\beta\cos\theta} \qquad (1)$$

where d is the grain size, λ is the X-ray wavelength, β is the line width at one-half the maximum intensity, and θ is the diffraction angle. It should be noted that no lattice strain effects are considered during the grain size calculation because the nanocrystalline composite powders in the present study are produced by gas-phase evaporation, different a lot from the nanocrystalline W–Ni–Fe composite powder synthesized by mechanical alloying process with large lattice distortion, supersolidus solution and amorphous phase [22,23]. Hence, according to Scherrer equation, the calculated tungsten grain sizes of 93W–4.9Ni–2.1Fe and 93W–4.9Ni–2.1Fe–0.03Y powders are about 40–50 nm and 20–30 nm, respectively. Note that the tungsten grain size of 93W–4.9Ni–2.1Fe powders is larger than that of 93W–4.9Ni–2.1Fe–0.03Y powders, indicating significant grain refinement caused by the addition of trace yttrium. Our previous work [24] indicated that the Y_2WO_6 compound was formed during hydrogen reduction process by adding 5 wt.% yttrium, and this compound effectively decreased the tungsten grain size of nanocrystalline composite powders through inhibiting the evaporation–sedimentation of tungsten-oxide in hydrogen reduction process. In this work, however, Y_2WO_6 diffraction peaks are absent in the XRD patterns due to the small amount of this compound in the nanocrystalline composite powders.

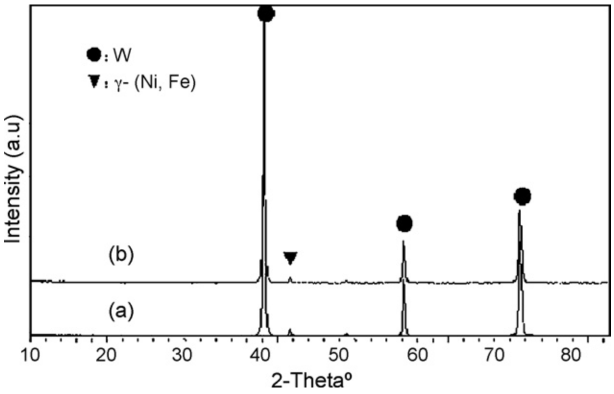

Fig. 1. XRD patterns of nanocomposite powders obtained by sol-spray drying and hydrogen reduction process:(a) 93W–4.9Ni–2.1Fe; (b) 93W–4.9Ni–2.1Fe–0.03Y.

The SEM images in Fig. 2 show the morphology of the nanocrystalline composite powders. It can be seen that both powders have a spherical shape and uniform particle size. Agglomeration is also observed in these powders, resulting from the large surface area of the small particles. However, the degree of agglomeration in nanocrystalline 93W–4.9Ni–2.1Fe–0.03Y composite powders is much lower than that in the nanocrystalline 93W–4.9Ni–2.1Fe composite powders. The reason may be that the Y_2WO_6 compounds are homogeneously adsorbed on the surfaces of these nanosized particles and significantly reduce the surface activity.

3.2. Sintering densification and microstructure evolution of nanocrystalline 93W–4.9Ni–2.1Fe composite powders

Fig. 3 plots the sintering density of 93W–4.9Ni–2.1Fe compacts versus sintering temperature at different holding time. It can be seen that the density increases gradually when the sintering temperature increases from 1320 °C to 1410 °C and nearly full density (17.646 g/cm^3) is obtained at 1410 °C for 1 h (the theoretical density is 17.735 g/cm^3). When the sintering temperature is above 1410 °C, the fully dense compacts are subject to density degradation with increasing sintering temperature. The trend of density degradation becomes more obvious as the holding time increases. For instance, the sintering density of the 93W–4.9Ni–2.1Fe compacts decreases